Separation Science and Technology
Publication details, including instructions for authors and subscription information:
http://www.informaworld.com/smpp/title~content=t713708471

Properties of Hollow Fibers Used for Flow Field-Flow Fractionation

Alf Carlshaf[a]; Jan Åke Jönsson[a]
[a] DEPARTMENT OF ANALYTICAL CHEMISTRY, UNIVERSITY OF LUND, LUND, SWEDEN

To cite this Article Carlshaf, Alf and Jönsson, Jan Åke(1993) 'Properties of Hollow Fibers Used for Flow Field-Flow Fractionation', Separation Science and Technology, 28: 4, 1031 — 1042
To link to this Article: DOI: 10.1080/01496399308029236
URL: http://dx.doi.org/10.1080/01496399308029236

SEPARATION SCIENCE AND TECHNOLOGY, **28**(4), pp. 1031–1042, 1993

Properties of Hollow Fibers Used for Flow Field-Flow Fractionation

ALF CARLSHAF and JAN ÅKE JÖNSSON*
DEPARTMENT OF ANALYTICAL CHEMISTRY
UNIVERSITY OF LUND
P.O. BOX 124, S-22100 LUND, SWEDEN

Abstract

An objective method for evaluating the suitability of different hollow fibers as separation channels in hollow-fiber flow-FFF is presented. The method is applied to evaluate four different fiber types and to compare several fibers of the same type. It is shown that the maximum plate number achievable with a certain fiber is governed by the homogeneity of the distribution of pores in the fiber wall. The method makes it possible to distinguish and measure the contribution to the peak width that originates from the inhomogeneity in pore distribution.

INTRODUCTION

Flow field-flow fractionation, one of the subtechniques in the field-flow fractionation family (*1*, *2*), is in principle the most versatile of all the different types of FFF yet investigated. The most used technique, however, is sedimentation FFF. Flow-FFF has not yet been developed for easy use as a standard technique.

There are several critical parameters that must be controlled in an exact way to perform a successful FFF separation. For instance, it is necessary that the walls of the separation channel be smooth and that the flows can be controlled in a precise way. Accurate control of the axial and radial flows in the channel where the separation takes place are crucial to predict retention and dispersion data for a solute of known particle size. It is also vital that the geometry of the separation channel is defined and constant. In the case of the classical parallel plate configuration, the walls must be absolutely parallel to maintain the desired parabolic flow profile in the

*To whom correspondence should be addressed.

axial direction. This is more difficult to achieve for flow-FFF than for most other FFF subtechniques because the channel walls must be porous to permit passage of the cross-flow (*3*). In the so-called asymmetrical flow-FFF technique (*4*), only one of the walls is porous, simplifying the construction. In all cases the channel wall porosity must be homogeneous throughout the whole channel to obtain a defined and known cross-flow profile.

We have presented an alternative version of flow-FFF (*5*), in which the parallel-plate arrangement is exchanged for a cylindrical porous tube (hollow fiber). This permits technically simple construction of a separation channel with defined geometry, as a pressurized flexible tube will automatically tend to form a perfect cylindrical cross section. Also, the connection of the channel to the rest of the equipment is simple, avoiding special endpieces that could possibly introduce flow disturbances. With the set-up used, the flows can be controlled independently, which permits gradient elution in a technically simple way (*6*).

In flow-FFF the majority of the particles to be separated are located less than a few micrometers from the channel wall. Because of this, the flow conditions close to the wall are crucial, necessitating an extremely smooth surface. The only suitable hollow fibers for FFF are of the anisotropic type (i.e., with a smooth skinlike inner surface and a coarser outer supporting structure). Other types of hollow fibers, including porous glass capillaries (*7*), have a mcirostructure that is too rough.

The theory for hollow fiber flow-FFF (*5*) can be used to predict the retention time and peak dispersion for a sample with known particle size. Provided that the ionic strength of the elution medium is properly adjusted (*8*), the theoretically predicted data agree well with experimental results in the case of retention time, but not so well for dispersion. We believe that this deviation is mainly caused by inhomogeneities in the porosity of the fiber wall. If the wall consists of some segments with high porosity and other segments with less porosity, this will not have any significant influence on the total retention time but will obviously have a band-broadening effect on a sample peak.

Commercially available anisotropic fibers are produced for the purpose of industrial-scale filtration and are comparatively low-priced. If the permeability in different segments of the fiber varies slightly, this will have no adverse effect on the intended industrial use. The suitability for use in FFF, however, will be determined by this property. Within a batch there are individual fibers with more or less homogeneous porosity, and those are consequently more or less suitable as separation channels. In this paper we present an objective method to evaluate and compare the homogeneity of the porosity of different hollow fibers.

EXPERIMENTAL

The hollow-fiber flow-FFF system was previously described in detail (*5, 6*). Briefly, it is based on the FPLC range of liquid-chromatographic equipment (Pharmacia LKB, Uppsala, Sweden). The hollow fibers investigated, listed in Table 1, were encapsulaed in an empty, modified column tube (Model C 16, Pharmacia). Sample was injected with an internal volume injection valve (Model 7410, Rheodyne Inc., Cotati, California, USA) equipped with a pneumatic actuator unit. The injection volume was 1 μL in all experiments with latex beads and 5 μL in the experiments with proteins. The detector was a fixed wavelength (254 nm) UV detector (UV-1, Pharmacia). The axial and the radial liquid flows were created by two syringe pumps (Model P-500, Pharmacia) connected to the fiber. The pumps were further connected to a computerized control unit (LCC500, Pharmacia) which was programmed to control the pumps independently as well as the injection valve.

The method for evaluating the homogeneity of pore size and pore distribution in a hollow fiber was tested with polystyrene latex beads (Sigma Chemical Company, St. Louis, Missouri, USA). The particle diameter was 0.091 μm with a standard deviation of 0.0058 μm. A buffer solution of 0.01 M Tris-HCl containing 1 mM EDTA, 0.1% Triton X-100, 100 mM NaCl, and 0.04% NaN_3 at pH 7.4 was used for the Harp and A/G fibers. For the Amicon fiber, water solutions of 0.1% Triton X-100 and varying concentrations of NaCl were used. All chemicals were of analytical grade, and the water was purified using a Milli-Q/RO-4 unit (Millipore, Bedford, Massachusetts, USA).

The polystyrene particles were diluted in the elution media (0.2% solid content) and the suspension was sonicated about 1 hour before use to

TABLE 1
Fibers Investigated

Fiber type	Brand	Model number	i.d. (mm)	MW cutoff (Dalton)
A	Harp[a]	HF1.0-60-PM50	1.5	50,000
B	Harp[a]	HF1.0-43-PM100	1.1	100,000
C	Amicon[b]	H5P100-43	1.1	100,000
D	A/G[c]	UFP-100-E-6	1.0	100,000

[a]Supelco, Inc., Bellefonte, Pennsylvania, USA (produced by Romicon, Inc., Woburn, Massachusetts, USA).

[b]Amicon Corp., Danvers, Massachusetts, USA.

[c]A/G Technology Corp., Needham, Massachusetts, USA.

disrupt particle aggregates. To ensure that no reaggregation occurs, the sonication was repeated every 4 hours.

To investigate the maximum plate number, the protein ferritin was used (Gel Filtration Calibration Kit, Pharmacia LKB, Uppsala, Sweden). A buffer solution of 0.01 M Tris-HCl containing 1 mM EDTA, 100 mM NaCl, and 0.04% NaN_3 at pH 9.0 was used both as diluent for the protein (35 mg/mL) and as eluent.

The evaluation of plate numbers was made graphically in all cases from the retention time and width at half height. For very low plate numbers, as sometimes encountered in this work, the procedure is of limited accuracy, but this is of little importance for the conclusions drawn.

THEORY

A cylindrical tube with a permeable wall, having a homogeneous distribution of pores, will cause the dispersion (plate number n) and retention time t_R of an ideally injected sample plug to follow the equations given earlier (5):

$$t_R = \frac{R^2}{8D} \ln (\bar{u}_z(0)/\bar{u}_z(L)) \tag{1}$$

$$n = \frac{\overline{Pe}^2}{32} \ln (u_z(0)/u_z(L)) \tag{2}$$

$$\overline{Pe} = \bar{u}_R R/D \tag{3}$$

where u_z and u_R are the linear axial and radial flows, respectively, $\overline{Pe}$ is the average Peclet number, R is the fiber radius, L is the fiber length, and D is the particle diffusion coefficient.

A real hollow fiber can be imagined to consist of patches with different porosities. This will cause the injected particles to experience a high radial flow in some parts of the fiber and a lower radial flow in othes. Thus, the retention of a single particle will vary accordingly, which increases the peak broadening. The total retention time, however, will not be influenced because it is determined by the mean radial flow rate. This is controlled by a separate pump and is independent of the homogeneity of porosity.

To quantify the increase in peak broadening arising from inhomogeneity of the porosity, the total observed variance σ^2_{obs} of an experimental peak is expressed as the sum of variances arising from various independent broadening mechanisms:

$$\sigma^2_{obs} = \sigma^2_{parab} + \sigma^2_{ax} + \sigma^2_{inf} + \sigma^2_{ext} + \sigma^2_{poly} + \sigma^2_{inhom} \tag{4}$$

where the subscripts signify, respectively, broadening arising from the parabolic flow profile, from axial diffusion, from the width of the focused injection plug, from external connections (including the detector cell), from the polydispersity of the sample particle size and, finally, from the inhomogeneity of channel wall porosity.

The contribution from the parabolic flow profile σ^2_{parab} corresponds to the ideal peak broadening effect, which can be calculated from the retention time and plate number in the ideal case (Eqs. 1–3):

$$\sigma^2_{parab} = t_R^2/n \tag{5}$$

This gives the expression for the contribution from the parabolic flow profile:

$$\sigma^2_{parab} = \frac{R^2}{2\overline{u_R^2}} \ln (u_z(0)/u_z(L)) \tag{6}$$

The contribution from axial diffusion σ^2_{ax} is usually insignificant for the sample types that are of interest for FFF. It can be calculated (in time units) by Einstein's equation:

$$\sigma^2_{ax} = \left(\frac{t_R}{L}\right)^2 2Dt = \frac{t_R^3}{L^2} 2D \tag{7}$$

In Eq. (7), t is the diffusion time, in this case equal to the retention time t_R.

The sum of the contributions from injection band width σ^2_{inj} and from external sources σ^2_{ext} can be estimated from experiments with no retention, i.e., with no radial flow. The experiments give an upper limit for these contributions, which are found to be negligible in comparison with the other contributions. Experiments with molecules with molecular weights close to the fiber exclusion limit and normal radial flows give similar results.

Finally, the polydispersity contribution σ^2_{poly} can be neglected if a monodisperse sample is used. However, most particle samples are not monodisperse, especially not samples of industrial origin like polystyrene latex beads. Also biomolecules, such as proteins or plasmides which are usually not rigid, show some polydispersity. If the polydispersity is known, the corresponding variance contribution can be calculated because the retention time is proportional to particle diameter.

$$\sigma^2_{poly} = \left(\frac{s_d}{m_d} t_R\right)^2 \tag{8}$$

In Eq. (8), m_d and s_d are the mean and the standard deviation of the particle diameters, respectively.

From the variance of an experimentally obtained peak, the calculated or estimated contributions can be subtracted. The resulting residual variance, σ_r^2, can then be attributed to be caused by inhomogeneity of porosity. There is, however, a possibility that the observed remainder is at least partially caused by another, unforeseen mechanism. To facilitate conclusions about this, we may observe that the variance contribution from porosity inhomogeneity should have the following characteristics:

- In a single fiber, the relative influence of this mechanism must be the same for all flow rates. The relative variation of the radial flow rate caused by variations in porosity will be independent of the flow rate and will influence all sample compounds in the same way. Thus the quotient σ_{inhom}/t_R should be independent of the flow rates.
- There may well be differences between individual fibers of the same type in this respect, and such differences are expected.
- Between various types of fibers, the differences may be still larger.

Other possible contributions to the variance, originating from causes other than the fiber porosity variation, should be of a more general nature, and not linked to individual fibers.

RESULTS AND DISCUSSION

Using several types of hollow fibers (Table 1), the retention time and peak width for polystyrene beads were measured at two different cross-flow conditions for five individual fibers of each type. The residual peak variance σ_r^2 was calculated as described above. The results are summarized in Tables 2–5 as the dimensionless quotient σ_r/t_R.

As an example, the calculation for the first fiber of type A was made as follows: The measured retention time was 23.2 min and the plate number n calculated from the width at half height was 119.5. From this is calculated the observed variance $\sigma_{obs}^2 = t_R^2/n = 4.5$ min^2. σ_{poly}^2 is found to be 2.19 min^2 from Eq. (8). σ_{parab}^2 was calculated from Eq. (6), giving the result 1.76 min^2. The axial diffusion term σ_{ax}^2 was calculated from Eq. (7) ($\approx 10^{-4}$). Finally, the sum of σ_{inj}^2 and σ_{ext}^2 was estimated from experiments without cross-flow ($\approx 10^{-3}$). By subtraction, σ_r^2, was found to be 0.55 min^2.

The precision was evaluated using a fiber (#5) of type C and a cross-flow rate of 0.10 mL/min. Ten repetitive measurements gave the following results: $t_R = (23.40 \pm 0.33)$ min (95% confidence interval) and $\sigma_r/t_R = (5.10 \pm 0.23)\%$.

TABLE 2
Results for Fiber Type A (Harp HF1.0-60-PM50)

Fiber	Cross-flow[a] (mL/min)	t_R (min)	σ^2_{obs} (min^2)	σ_r/t_R (%)	σ_r/t_R (mean)
1	0.14	23.2	4.5	3.2	3.7
		23.6	4.9	3.9	
	0.20	36.8	9.3	4.3	
		37.0	8.4	3.3	
2	0.14	22.0	4.9	4.8	4.2
		22.4	4.9	4.5	
	0.20	35.5	8.3	3.9	
		36.0	8.3	3.7	
3	0.14	23.6	4.4	2.9	3.4
		24.2	4.7	3.1	
	0.20	37.0	8.8	3.8	
		37.2	8.8	3.7	
4	0.14	22.0	4.5	4.0	4.2
		22.0	4.2	4.0	
	0.20	34.8	8.3	4.2	
		35.2	8.8	4.5	
5	0.14	22.2	5.6	6.2	5.6
		22.2	5.2	5.5	
	0.20	34.8	9.3	5.1	
		35.2	10.4	5.7	

[a]The axial flow was 1.60 mL/min in all cases.

Several observations can be made from the material in Tables 2–5:

- σ_r/t_R varies considerably in the range 1.3 to 13%.
- Repetitive measurements on the same fiber yield very similar results for different flow conditions.
- There are clear differences between individual fibers in the same batch.

From these observations it can be concluded that at least the main part of the observed residual variance σ_r/t_R is caused by inhomogeneity of the porosity.

The values of σ_r/t_R are in many cases relatively high, which indicates a relatively high influence from porosity inhomogeneity. To achieve the high separation capability that is predicted by theory, this factor must be controlled and minimized. The lowest values were observed with two fibers

TABLE 3
Results for Fiber Type B (Harp HF1.0-43-PM100)

Fiber	Cross-flow[a] (mL/min)	t_R (min)	σ^2_{obs} (min^2)	σ_r/t_R (%)	σ_r/t_R (mean)
1	0.10	22.8	4.9	4.4	4.9
		22.4	4.9	4.6	
	0.14	34.0	9.3	5.3	
		34.0	9.3	5.3	
2	0.10	21.8	4.9	5.0	4.8
		21.6	4.9	5.1	
	0.14	31.6	7.4	4.4	
		32.2	7.8	4.7	
3	0.10	23.2	4.0	1.8	1.7
		23.4	4.2	1.7	
	0.14	34.4	6.5	1.7	
		34.2	6.5	1.7	
4	0.10	23.6	4.3	2.3	1.7
		23.6	4.2	1.5	
	0.14	34.8	6.5	1.3	
		34.6	6.5	1.5	
5	0.10	22.0	6.5	7.5	8.3
		21.8	6.5	7.6	
	0.14	32.0	14.0	9.1	
		32.6	14.0	8.8	

[a]The axial flow was 1.60 mL/min in all cases.

of type B, but, on the other hand, other fibers of the same type showed considerably worse values. For the other types, the variation was less dramatic. Thus, it is possible to find fibers of type B with good properties, but it is imperative that comparative tests be performed. Fibers of the other types are less variable, but generally less homogeneous.

With a fiber with $\sigma_r/t_R = 1.7\%$, which is the best value found (Table 3), the absolute maximum plate number obtainable is about 3500 (i.e., $1/0.017^2$). This plate number would be found under conditions where all other peak broadening mechanisms become insignificant compared to that due to the membrane porosity. With a "bad" value of $\sigma_r/t_R = 10\%$, it is thus impossible to obtain larger plate numbers than 100, irrespectively of the magnitude of the controllable peak broadening sources and of the properties of the sample.

A relatively "good" fiber of type B (with $\sigma_r/t_R = 3.0\%$) was tested by injecting a protein (ferritin) and observing the plate number at different

TABLE 4
Results for Fiber Type C (Amicon H5P100-43)

Fiber	Cross-flow[a] (mL/min)	t_R (min)	σ^2_{obs} (min^2)	σ_r/t_R (%)	σ_r/t_R (mean)
1	0.10	22.0	6.5	7.5	8.0
		22.0	6.5	7.5	
	0.14	29.6	11.5	8.7	
		30.4	11.5	8.3	
2	0.10	22.8	6.5	7.1	7.1
		22.6	6.5	7.2	
	0.14	32.6	11.5	7.4	
		33.0	10.4	6.5	
3	0.10	22.4	4.9	4.6	5.1
		23.6	5.6	5.4	
	0.14	32.2	7.6	4.4	
		32.8	9.3	5.8	
4	0.10	21.0	4.9	5.4	5.7
		21.0	4.9	5.4	
	0.14	30.0	8.3	6.1	
		31.2	8.8	6.0	
5	0.10	23.2	5.3	4.9	5.0
		23.6	5.9	5.2	
	0.14	30.8	7.4	4.8	
		31.0	7.8	5.2	

[a]The axial flow was 0.60 mL/min in all cases.

radial flows. The plate number should be limited by the inhomogeneity of porosity to approximately 1100 $[(1/0.03)^2]$ for a mono-dispersed sample and negligible peak broadening by the parabolic flow profile. Examples of fractograms are shown in Fig. 1. Two additional peaks, probably protein impurities, can be seen after the main peak. At all radial flows the second of these has a retention time that corresponds to a Stokes diameter of 22 nm. The plot in Fig. 2 shows the plate number for this peak at five different radial flows. Assuming, as is often done, that the theoretical plate number is fully accounted for by the variance due to the parabolic flow profile, which according to Eq. (6) is strongly reduced at high radial flows, n for the lowest radial flow (0.7 mL/min) would be 2800 and for the highest (1.2 mL/min) 20,000. It is clearly seen that the curve asymptotically approaches the 1100 plates, as expected.

The value of σ_r/t_R varied between 3.1 and 3.5% for the five different radial flows. The slightly increased values of σ_r/t_R probably originates from

TABLE 5
Results for Fiber Type D (A/G UFP-100-E-6)

Fiber	Cross-flow[a] (mL/min)	t_R (min)	σ^2_{obs} (min^2)	σ_r/t_R (%)	σ_r/t_R (mean)
1	0.09	14.4	3.5	8.0	8.0
		14.4	3.3	7.5	
	0.13	21.6	6.5	8.8	
		21.6	5.6	7.7	
2	0.09	16.8	2.9	3.8	3.6
		16.8	2.9	3.8	
	0.13	26.8	4.9	3.7	
		26.4	4.5	3.1	
3	0.09	13.3	3.5	9.0	9.2
		12.6	3.3	9.3	
	0.13	20.0	5.6	8.7	
		20.0	6.5	9.8	
4	0.09	17.0	3.5	5.9	6.3
		16.8	3.8	6.9	
	0.13	27.6	6.5	5.6	
		27.4	7.4	6.7	
5	0.09	17.2	4.5	8.2	9.8
		17.2	4.5	8.2	
	0.13	22.0	7.4	9.6	
		21.2	10.4	13.0	

[a]The axial flow was 0.60 mL/min in all cases.

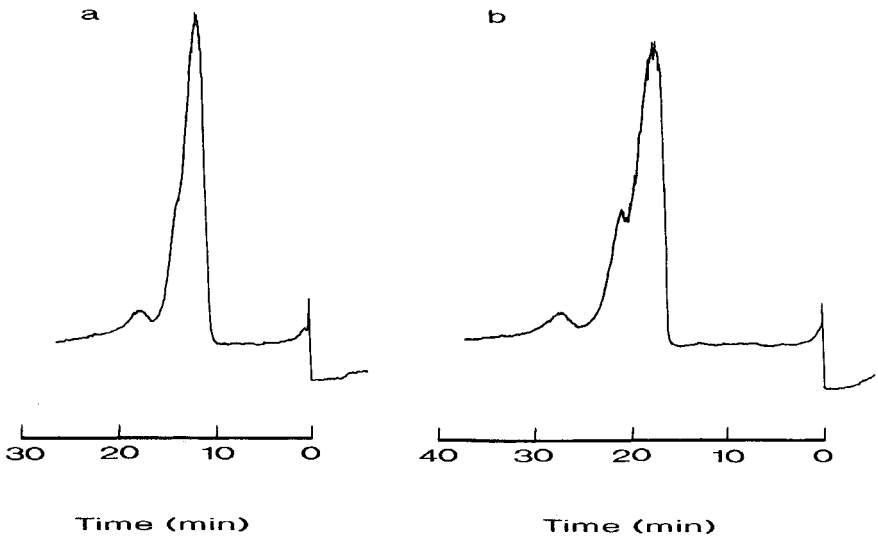

FIG. 1. Fractograms of ferritin (0.18 mg) with two impurity peaks. The separation channel was of type B (length: 24 cm, inner diameter: 1.1 mm). Flow conditions, axial flow and radial flow, respectively: (a) 1.5 and 0.7 mL/min, (b) 1.5 and 0.9 mL/min.

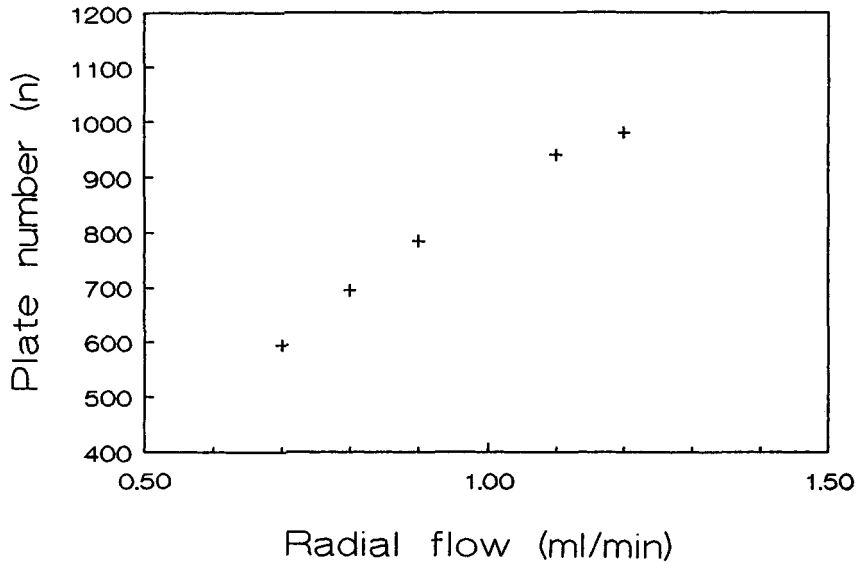

FIG. 2. Plate number (n) versus the radial flow for the second inpurity peak in the fractograms of ferritin. The axial flow was 1.5 mL/min in all runs. Injection volume was 5 μL and the total protein concentration was 35 mg/mL.

some polydispersity of the sample, which according to these measurements corresponds to a relative standard deviation of approximatively 1–2%.

The measurements and calculations described here can be used to compare various brands and types of hollow fibers and to choose suitable fibers in an objective way. It is also shown that the efficiency of a separation and the absolute maximum plate number achievable strongly depends on the pore distribution in the channel.

Acknowledgment

This work was supported by the Swedish Natural Science Research Council.

REFERENCES

1. J. Janca, *Field-Flow Fractionation: Analysis of Macromolecules and Particles,* Dekker, New York, 1988.
2. K. D. Caldwell, *Anal. Chem.*, **60,** 959A (1988).
3. K. G. Wahlund, H. S. Winegartner, K. D. Caldwell, and J. C. Giddings, *Ibid.*, **58,** 573 (1986).

4. K. G. Wahlund and J. C. Giddings, *Ibid.*, **59,** 1332 (1987).
5. J. Å. Jönsson and A. Carlshaf, *Ibid.*, **61,** 11 (1989).
6. A. Carlshaf and J. Å. Jönsson, *J. Chromatogr.*, **461,** 89 (1989).
7. R. Schnabel and P. Langer, *Glastech. Ber.*, **62,** 56 (1989).
8. A. Carlshaf and J. Å. Jönsson, *J. Microcolumn Sep.*, **3,** 411 (1991).

Received by editor November 13, 1991
Revised June 26, 1992